Electronic Supplementary Information

Nickel coordination polymer derived from 1,2,4,5-tetraaminobenzene for fast and stable potassium battery anodes

Roman R. Kapaev,*[abc] Ivan S. Zhidkov,[d] Ernst Z. Kurmaev,[de] Keith J. Stevenson,[a] Pavel A. Troshin[ab]

[a] Center for Energy Science and Technology, Skolkovo Institute of Science and Technology, Nobel str. 3, Moscow 143026, Russia. E-mail: roman.kapaev@skoltech.ru
[b] Institute for Problems of Chemical Physics RAS, Acad. Semenov str. 1, Chernogolovka 142432, Russia
[c] D.I. Mendeleev University of Chemical Technology of Russia, Miusskaya sq. 9, Moscow 125047, Russia
[d] Institute of Physics and Technology, Ural Federal University, Mira str. 19, Yekaterinburg 620002, Russia
[e] M.N. Mikheev Institute of Metal Physics of Ural Branch of Russian Academy of Sciences, S. Kovalevskoi str. 18, Yekaterinburg 620108, Russia

Experimental procedures

Electrode preparation: active material (**P1**), Super P and carboxymethyl cellulose sodium salt with weight ratios of 60:30:10 or 80:10:10 were thoroughly mixed in deionized water to form a homogeneous slurry, which was then tape-cased onto aluminium foil, vacuum-dried at 110 ˚C for 10 h, calendered at room temperature and vacuum-dried again at 110 ˚C for 5 h. Composite mass loading was ~1.7 mg cm^{-2} (**P1** mass loading ~1 mg cm^{-2}) for the electrode with 30% wt. Super P and ~1.6, ~5.0 or 15.2 mg cm^{-2} for the electrodes with 10% wt. Super P. To estimate the contribution to the capacity from Super P, an electrode containing only Super P and carboxymethyl cellulose sodium salt (weight ratio Super P:CMC = 70:30) was prepared according to the same procedure; Super P mass loading for this electrode was ~0.5 mg cm^{-2}.

Cell assembling and testing: Coin cells (CR2032-type) were assembled in a dry argon-filled glovebox with oxygen level below 1 ppm. 1.5ᴍ solution of KPF_6 in dry 1,2-dimethoxyethane was used as an electrolyte, potassium metal was used as an anode, glass fiber (Whatman GF/A Glass microfiber filters, GE Healthcare) was used as a separator. Galvanostatic cycling was performed with Neware battery testing systems, cyclic voltammetry was carried out with BioLogic VMP3 potentiostat. Voltage window was 0.5–2.0 V for all cells.

Calculations: Both specific capacities and current densities were calculated basing on the mass of active materials (**P1** for **P1**-based electrodes, Super P for electrodes without **P1**). Coulombic efficiency was calculated as the ratio between charge and discharge capacities.

For **P1**-based electrodes, capacity contribution of Super P (Fig. S1) was subtracted. To do so, charge-discharge curves of Super P at a given current rate were subtracted from the curves of **P1**-based electrodes at the same current rate, considering that the capacity of Super P is proportional to its content in the electrodes.
Particularly, the specific capacity of **P1** (Q_{P1}) was calculated as follows:

$$Q_{P1} = Q^*_{P1} - \frac{w_{SP}}{w_{P1}} Q_{SP}$$

where Q^*_{P1} is the capacity at a given current rate before the subtraction (i.e. absolute battery capacity in mA h divided by the mass of **P1**), Q_{SP} is the capacity of Super P at a given current rate (determined experimentally, calculated per the mass unit of Super P, see Fig. S1), w_{P1} and w_{SP} are weight percentages of **P1** and Super P in the electrodes, respectively (60 and 30 or 80 and 10, depending on the electrode composition).

Since **P1** and Super P have different charge-discharge profiles, it should be noted that the presence of Super P in the electrodes distorts the charge-discharge curves of **P1**. To distinguish the true charge-discharge profiles of **P1**, the following was done:

1. Each charge or discharge curve of **P1** or Super P was represented as an array of XY-pairs, with the potential (ranging from 0.5 to 2.0 V) being the X dimension and the capacity (Q^*_{P1} or $Q_{SP} \times w_{SP} \div w_{P1}$) being the Y dimension.
2. For each pair of arrays (attributed **P1** and Super P), reference subtraction, i.e. subtraction of one curve from another, was performed using OriginPro 2019. The information about the procedure is available at https://www.originlab.com/doc/X-Function/ref/subtract_ref. The Super P arrays were used as the references.
3. X and Y dimensions of the resulting arrays were swapped.

The curves before and after the subtraction are shown in Fig. S2.

In-situ XRD cell preparation and measurements: to prepare the electrode for XRD studies, active material, Super P and poly(vinylidene difluoride) with a weight ratio of 70:20:10 were thoroughly mixed in N-methylpyrrolidone to form a homogeneous slurry, which was then tape-cased onto aluminium foil, vacuum-dried at 110 ˚C for 10 h, calendered at room temperature and vacuum-dried again at 110 ˚C for 5 h. Composite mass loading was ~11 mg cm^{-2} (**P1** mass loading ~7.5 mg cm^{-2}). A Swagelok-type two-electrode cell with a beryllium window was assembled in a dry argon-filled glovebox with oxygen level below 1 ppm. Electrode with the studied material was placed next to the Be window (Al foil in contact with Be), 1.5ᴍ solution of KPF_6 in dry 1,2-dimethoxyethane was used as an electrolyte, potassium metal was used as an anode, glass fiber was used as a separator. XRD patterns were measured with Bruker ADVANCE D8 diffractometer, Cu Kα radiation, 2Θ range from 16˚ to 26˚, slit width 1 mm, step 0.06˚, time per step 10 s. The XRD patterns were measured continuously during galvanostatic discharge with the current density of 15 mA g^{-1}, which was performed with BioLogic SP-200.

XPS sample preparation and measurements: coin cells, which were charged/discharged at the current density 50 mA g^{-1}, were disassembled in the Ar-filled glovebox. The electrodes were washed with pure dry 1,2-dimethoxyethane and dried at room temperature. XPS was measured at PHI XPS 5000 VersaProbe spectrometer (ULVAC-Physical Electronics, USA) with a spherical quartz monochromator and an energy analyzer working in the range of binding energies (BE) from 0 to 1500 eV. The energy resolution was $\Delta E \leq 0.5$ eV. The samples were kept in the vacuum chamber for 24 h prior to the experiments and were measured at a pressure bellow 10^{-7} Pa. All spectra were calibrated for external reference Au $4f_{7/2}$ binding energies (84.1 eV). To study the active material itself rather than the SEI layer, Ar^+ ions with 500 eV energy (3 min) were used to eliminate upper SEI layers and reach the subsurface prior to measurements.

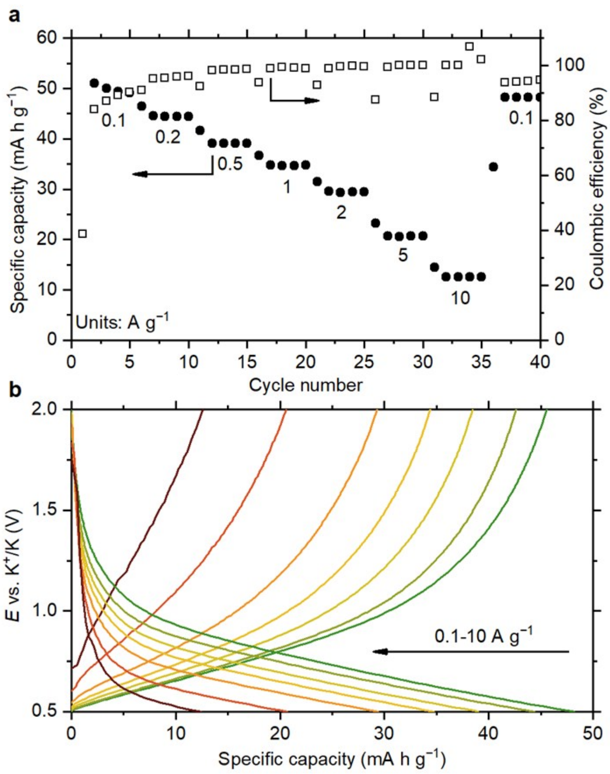

Fig. S1. Rate performance of Super P: (a) specific capacity for different current densities; (b) charge-discharge curves for each 5th cycle shown in (a) except for cycle 5.

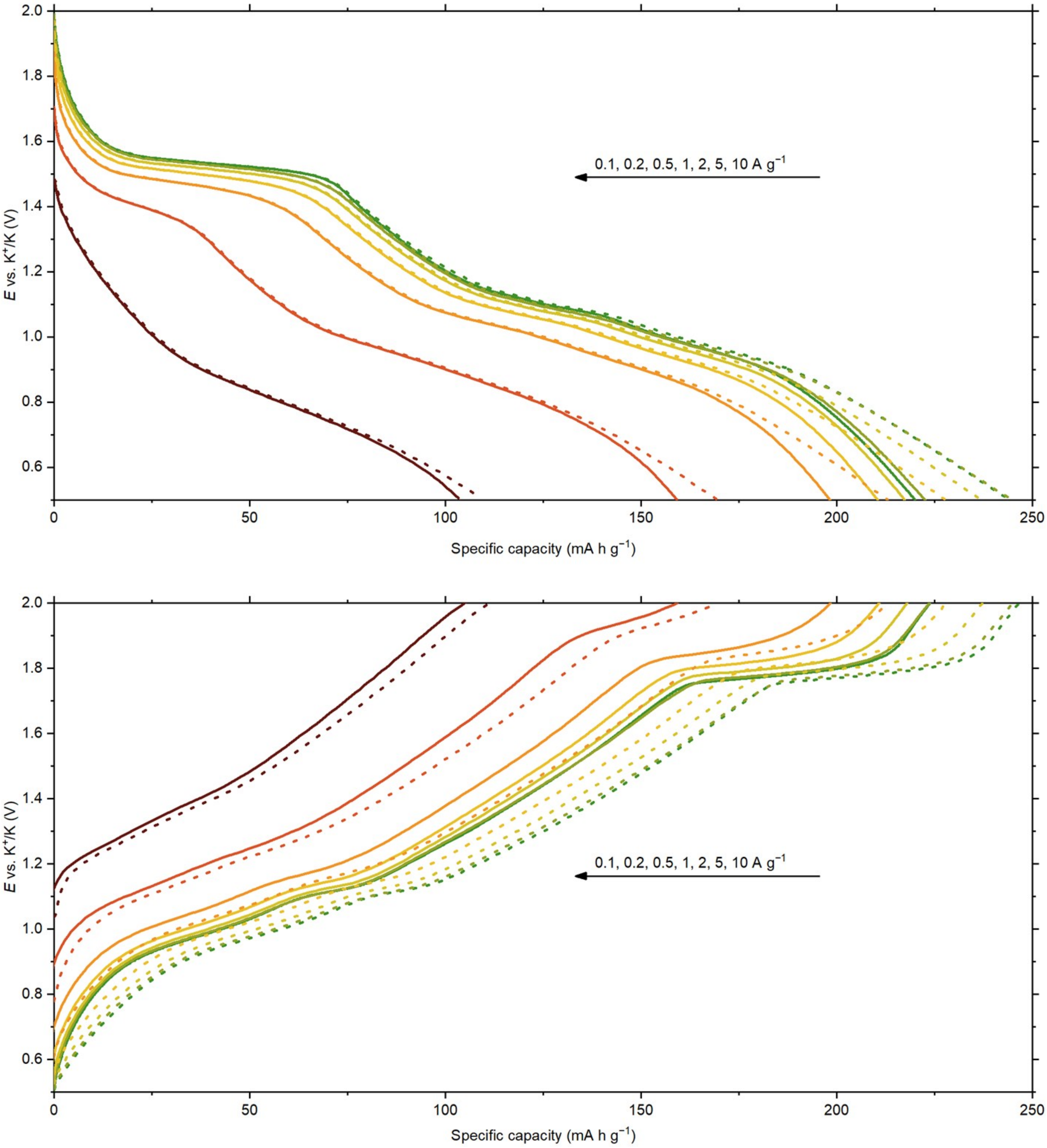

Fig. S2. Discharge (upper plot) and charge (lower plot) profiles at different current rates before (dotted lines) and after (solid lines) subtracting the contribution from Super P.

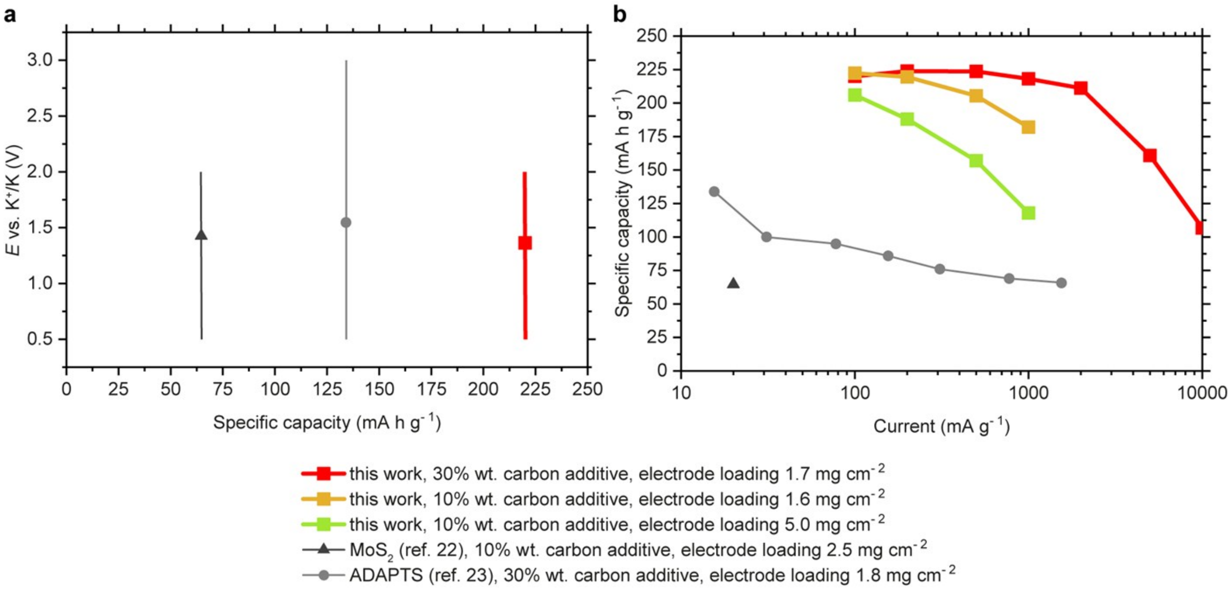

Fig. S3. (a) Working potentials and specific capacities of potassium battery anode materials operating above 0.5 V vs. K^+/K; voltage ranges are shown as lines and average depotassiation potentials are shown as scatter; (b) rate capabilities of the selected materials.

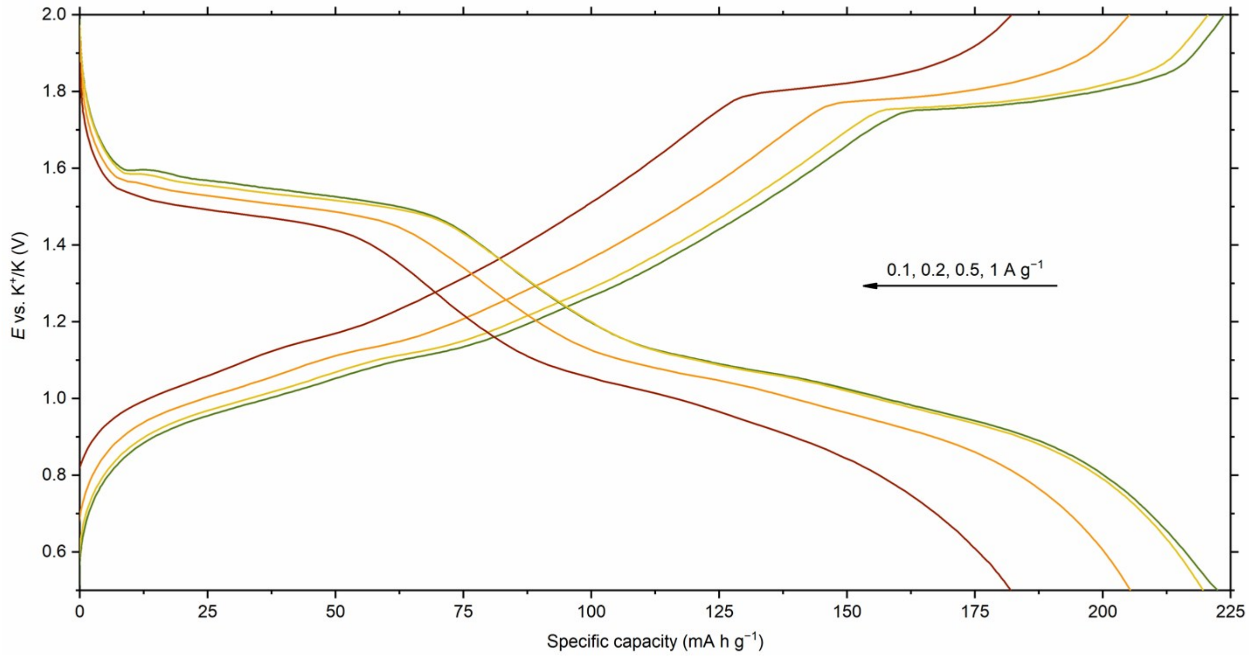

Fig. S4. Charge-discharge profiles of **P1** with 10% wt. Super P at different current densities. Contribution from Super P was subtracted.

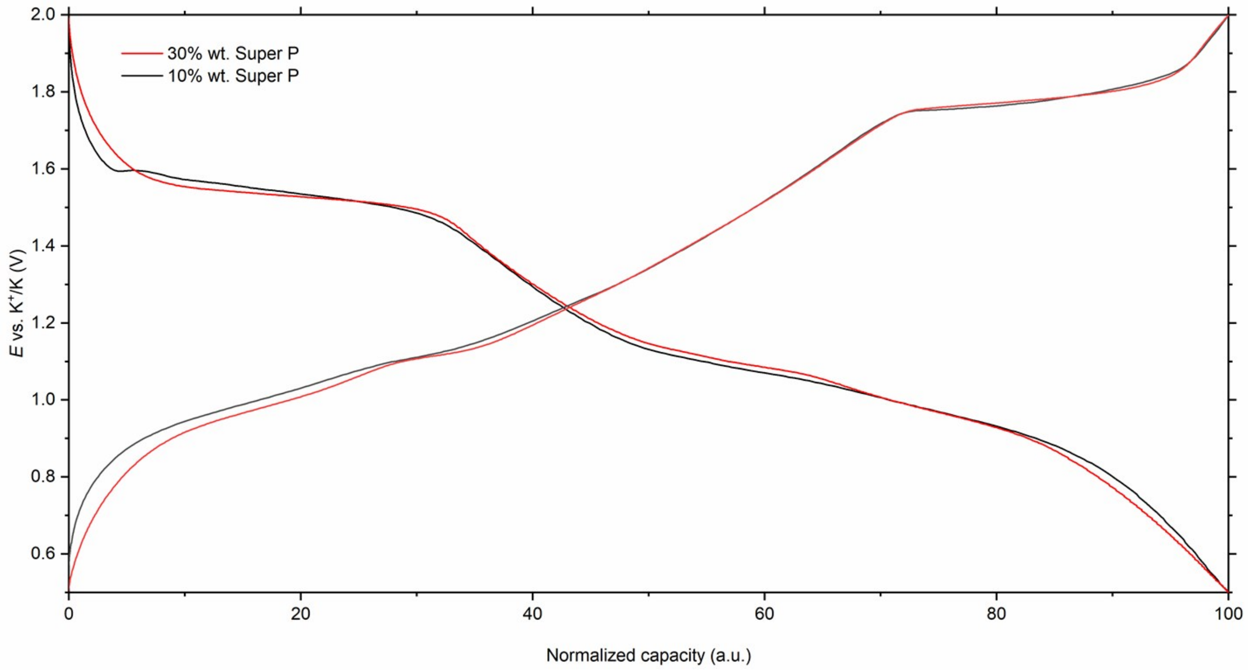

Fig. S5. Charge discharge profiles of **P1** with 10 and 30% wt. Super P at 0.1 A g^{-1}. Contribution from Super P was subtracted.

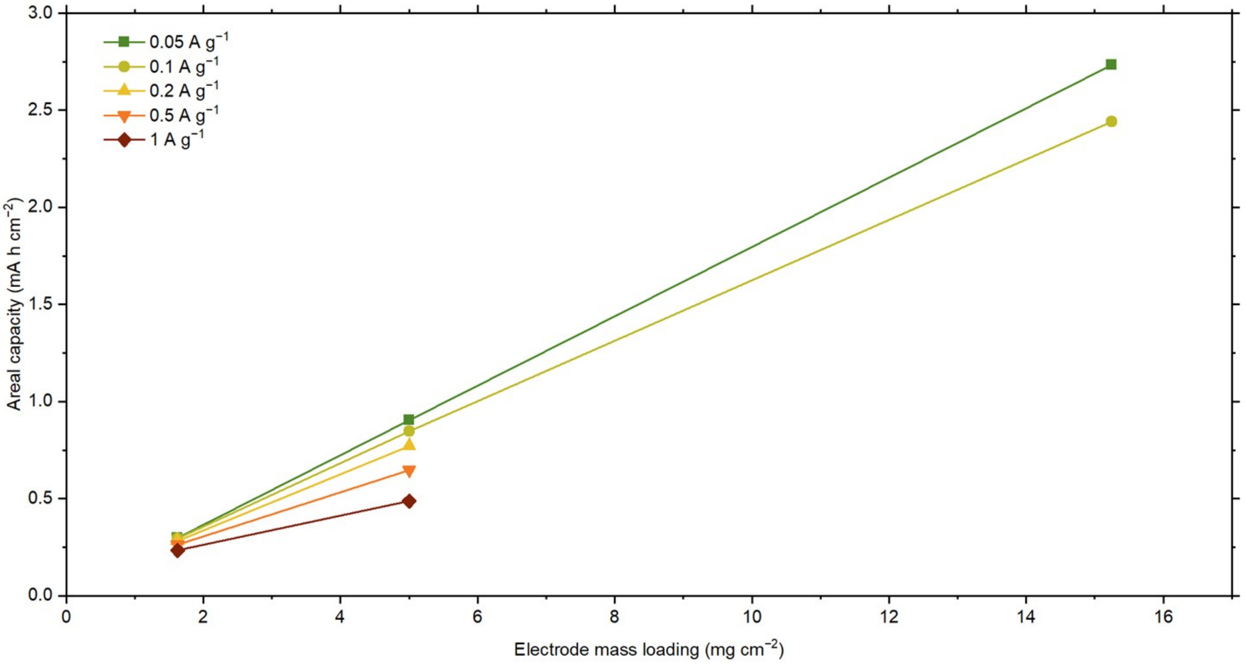

Fig. S6. Areal capacities of **P1**-based electrodes for different electrode loadings and current densities.